



# A flexible polypyrrole-coated fabric counter electrode for dye-sensitized solar cells



Jie Xu\*, Meixia Li, Lei Wu, Yongyuan Sun, Ligen Zhu, Shaojin Gu, Li Liu, Zikui Bai, Dong Fang, Weilin Xu\*

College of Materials Science & Engineering, State Key Laboratory for New Textile Materials & Advanced Processing Technology, Wuhan Textile University, 430200 Wuhan, China

## HIGHLIGHTS

- Conductive fabric with resistance of  $1.5 \Omega \text{ sq}^{-1}$  is achieved by Ni coating.
- Polypyrrole with sufficient electrocatalytic activity is synthesized on Ni-coated fabric.
- DSSCs fabricated using PPy/Ni-coated fabric counter electrode exhibit an efficiency of 3.30%.

## ARTICLE INFO

### Article history:

Received 22 September 2013

Received in revised form

4 January 2014

Accepted 28 January 2014

Available online 8 February 2014

### Keywords:

Dye-sensitized solar cell

Polypyrrole

Counter electrode

Conductive fabric

## ABSTRACT

The current dye-sensitized solar cell (DSSC) technology is mostly based on fluorine doped tin oxide (FTO) coated glass substrate. The main problem with the FTO glass substrate is its rigidity, heavyweight and high cost. DSSCs with a fabric as substrate not only offer the advantages of flexibility, stretchability and light mass, but also provide the opportunities for easy implantation to wearable electronics. Herein, a novel fabric counter electrode (CE) for DSSCs has been reported employing a daily-used cotton fabric as substrate and polypyrrole (PPy) as catalytic material. Nickel (Ni) is deposited on the cotton fabric as metal contact by a simple electroless plating method to replace the expensive FTO. PPy is synthesized by *in situ* polymerization of pyrrole monomer on the Ni-coated fabric. The fabric CE shows sufficient catalytic activity towards the reduction of  $\text{I}_3^-$ . The DSSC fabricated using the fabric CE exhibits power conversion efficiency of  $\sim 3.30\%$  under AM 1.5.

© 2014 Elsevier B.V. All rights reserved.

## 1. Introduction

Dye-sensitized solar cells (DSSCs) have attracted significant interests as promising alternatives for the photovoltaic conversion of solar energy due to their potentially low production costs and relatively high solar-to-electric conversion efficiencies [1–7]. Typically, DSSCs consist of a mesoporous dye-sensitized  $\text{TiO}_2$  photoanode, an iodide/triiodide ( $\text{I}^-/\text{I}_3^-$ ) redox electrolyte, and a counter electrode (CE). The CE plays an important role in DSSCs, which serves to collect electrons from external circuit and to catalyze  $\text{I}^-/\text{I}_3^-$  redox-coupled regeneration reaction in electrolyte.

Platinized fluorine-doped tin oxide (FTO) glass CE has been widely used in DSSCs due to its good electric conductivity and excellent catalytic activity for  $\text{I}_3^-$  reduction of platinum (Pt). However, large-scale commercial application of platinized CE is restricted by its high cost and high energy-consuming preparation (sputtering and thermal decomposition). Therefore, extensive studies have been carried out for the development of Pt-free CE in DSSCs. So far, many functional materials have been employed in Pt-free CE, such as carbon-based materials [8–11] and conducting polymers [12–18]. As a well-known conducting polymer, polypyrrole (PPy) has received more and more attention as a potential candidate for platinized CE because of its low cost, facile synthesis, high catalytic activity and remarkable environmental stability [14–18].

FTO glass is also one of the expensive components in DSSCs. The cost of conductive glass is estimated to account for about 30% of the total material cost of DSSCs [19]. Moreover, the rigid, fragile and

\* Corresponding authors.

E-mail address: [xujie0@ustc.edu](mailto:xujie0@ustc.edu) (J. Xu).

heavy-weight feature will bring transport problem for the FTO glass based DSSCs. Novel substrates such as metal foils or plastic foils coated with indium-doped tin oxide [20–22] have been used to fabricate flexible CE to achieve the requirements for portable electricity and high-throughput industrial roll-to-roll production. However, the cost of these flexible substrates is even much higher than that of FTO glass.

Fabrics are flexible and porous materials made by weaving or pressing fibers, which gives them important properties, such as flexibility, stretchability, and light mass. Among the fabrics, cotton (natural cellulose) is indeed the most commonly used material, because of its process easiness, relative cheapness and good mechanical properties. In this paper, we report a novel flexible CE employing a daily-used cotton fabric as substrate. Nickel (Ni) is coated on the cotton fabric as metal contact by a simple low temperature electroless plating method to replace the expensive FTO. The CE is prepared with PPy as catalytic material, which is synthesized by *in situ* polymerization of pyrrole monomer on the Ni-coated fabric. Fabric-based DSSCs are expected to meet the various requirements of electronic textiles and wearable electronics. In addition, the technologies for fabric coating are very mature in textile industries, which can benefit the roll-to-roll production of DSSCs on fabrics.

## 2. Experimental

### 2.1. Ni deposition on cotton fabrics

Plain weave 100% cotton fabrics ( $182 \text{ g m}^{-2}$ ) in white color were used as the substrates. Electroless nickel (Ni) plating was carried out by multi-step processes including pre-cleaning, activation, electroless Ni plating and post-treatment followed by rinsing and drying. In the pre-treatment stage, the fabric samples were pre-cleaned with a 5% non-ionic detergent at pH 7.0 and  $40^\circ\text{C}$  for 20 min. The samples were then rinsed with deionized water. Surface sensitization was conducted by immersing of the samples into an aqueous solution containing  $50 \text{ g L}^{-1}$  nickel sulfate ( $\text{NiSO}_4 \cdot 6\text{H}_2\text{O}$ ) and  $40 \text{ mL L}^{-1}$  38% hydrochloric acid (HCl) at  $25^\circ\text{C}$  for 10 min. The specimens were subsequently rinsed with deionized water and activated through immersion into a solution containing  $10 \text{ g L}^{-1}$  sodium borohydride ( $\text{NaBH}_4$ ) and  $10 \text{ g L}^{-1}$  sodium hydroxide (NaOH) at  $25^\circ\text{C}$  for 10 min. Then, the specimens were rinsed with a large volume of deionized water for more than 5 min to prevent contamination of the plating bath. After that, the activated specimens were coated via an autocatalytic reaction in the Ni-plating solution at  $70^\circ\text{C}$  for 2 h. The composition of the plating bath was as follows:  $25 \text{ g L}^{-1}$   $\text{NiSO}_4$ ,  $28 \text{ g L}^{-1}$  succinic acid ( $\text{C}_4\text{H}_6\text{O}_4$ ),  $20 \text{ g L}^{-1}$  DL-malic acid ( $\text{C}_4\text{H}_6\text{O}_5$ ) and  $25 \text{ g L}^{-1}$  sodium hypophosphite ( $\text{Na}_2\text{H}_2\text{PO}_2$ ). The pH of the plating bath was adjusted to 8.0 using NaOH aqueous solution. In the post-treatment stage, the Ni-coated fabrics were rinsed with deionized water at  $40^\circ\text{C}$  for 20 min immediately after the electroless nickel plating and then dried at  $60^\circ\text{C}$ .

### 2.2. Preparation of PPy/Ni-coated fabrics

The Ni-coated fabrics were immersed in an aqueous solution of pyrrole (1.0 M), cetyltrimethylammonium bromide (CTAB, 0.01 M) and sodium dodecyl benzene sulfonate (SDBS, 0.01 M) for 30 min under magnetic stirring. The polymerization was carried out at  $5^\circ\text{C}$  for 2 h by gently adding an aqueous solution of 0.5 M iron (III) chloride hexahydrate ( $\text{FeCl}_3 \cdot 6\text{H}_2\text{O}$ ) as oxidant agent to the stirred bath. The PPy/Ni-coated fabrics were then washed with deionized water and ethanol to extract the

byproducts and remaining reagents, and vacuum-dried at  $60^\circ\text{C}$  to constant weight.

### 2.3. DSSC fabrication

The  $\text{TiO}_2$  (P25, Degussa) paste was coated on FTO glass using the doctor-blade method with Scotch tape as the spacer. The  $\text{TiO}_2$  film was dried in air and sintered at  $450^\circ\text{C}$  for 1 h. The obtained  $\text{TiO}_2$  film had a thickness of  $\sim 10 \mu\text{m}$  and an area of  $\sim 0.36 \text{ cm}^2$ . The electrode was then immersed in a solution of 0.3 mM N719 (bis-(tetrabutylammonium)-cis-(dithiocyanato)-N,N'-bis(4-carboxylato-4'-carboxylic acid-2,2'-bipyridine) ruthenium, Solarnix) in ethanol for 24 h at room temperature. After that, the  $\text{TiO}_2$  electrode was rinsed thoroughly with ethanol and dried under a dry air stream. The DSSC was fabricated by sandwiching the sensitized  $\text{TiO}_2$  electrode and fabric CE using a sheet of stretched parafilm as the spacer. The backside of the cell was sealed by polymer film [23]. The electrolyte was injected between the photoanode and CE using a syringe. The electrolyte containing 0.6 M 1,2-dimethyl-3-propylimidazolium iodide (DMPPI), 0.025 M LiI, 0.04 M  $\text{I}_2$ , 0.05 M guanidium thiocyanate (GuSCN), and 0.28 M 4-tertbutylpyridine (TBP) in dry acetonitrile was used. The Pt CE was prepared by depositing a drop of 50 mM solution of  $\text{H}_2\text{PtCl}_6$  in isopropanol onto FTO substrates followed by annealing at  $450^\circ\text{C}$  in air for 15 min.

### 2.4. Characterization and measurement

The electrical conductivity of the samples was measured at room temperature by a four-point probe resistivity system (RTS-9, Probes Tech., China) with copper electrodes and a 5 N pressure at room temperature and relative humidity of 65%. The morphologies of the samples were examined by scanning electron microscopy (SEM, JSM-6510LV, JEOL, Japan). Double-sided conductive carbon tape was used to attach the samples to the microscope stage. The samples were sputtered with gold to get good electrical contact and avoid charging. The composition of the Ni-coated sample was examined using an energy dispersive spectrometer (EDS, EDAX, USA). Attenuated total reflection Fourier transform infrared (ATR-FTIR) spectra were recorded using a TGA-FTIR spectrometer (Tensor 27, Bruker, Germany) in the range from  $4000$  to  $600 \text{ cm}^{-1}$  with 8 scans and a resolution of  $2 \text{ cm}^{-1}$ . The Scotch tape test was performed; in this test a piece of Scotch tape is placed on the fabric and removed. The sample fails the test if any of it remains on the Scotch tape [24]. In order to test the corrosion resistance of Ni and PPy to electrolytes, the samples were immersed in electrolyte solution for 2 h and the transmittance of electrolytes was recorded by UV-2550 spectrometer (Shimadzu, Japan) before and after immersion. Less transmittance change of electrolytes is an indication of better corrosion resistance. The  $J$ - $V$  characteristics were measured under AM 1.5 simulated illumination (Sciencetech, SS150) with a power density of  $100 \text{ mW cm}^{-2}$ . Electrochemical impedance spectroscopy (EIS) measurements were carried out on Autolab PGSTAT302N (Metrohm AG, Switzerland) with the frequency ranging from 0.01 Hz to 100 kHz. For the EIS measurements, the symmetric cell configuration with two identical fabric or FTO CEs was used. The symmetric cell was constructed by sandwiching two identical CEs separated with a sheet of stretched parafilm. Two pieces of microscope glass were utilized to stabilize the fabric cell. The cell was sealed in polymer pouches. The same electrolyte for the DSSC fabrication was injected.

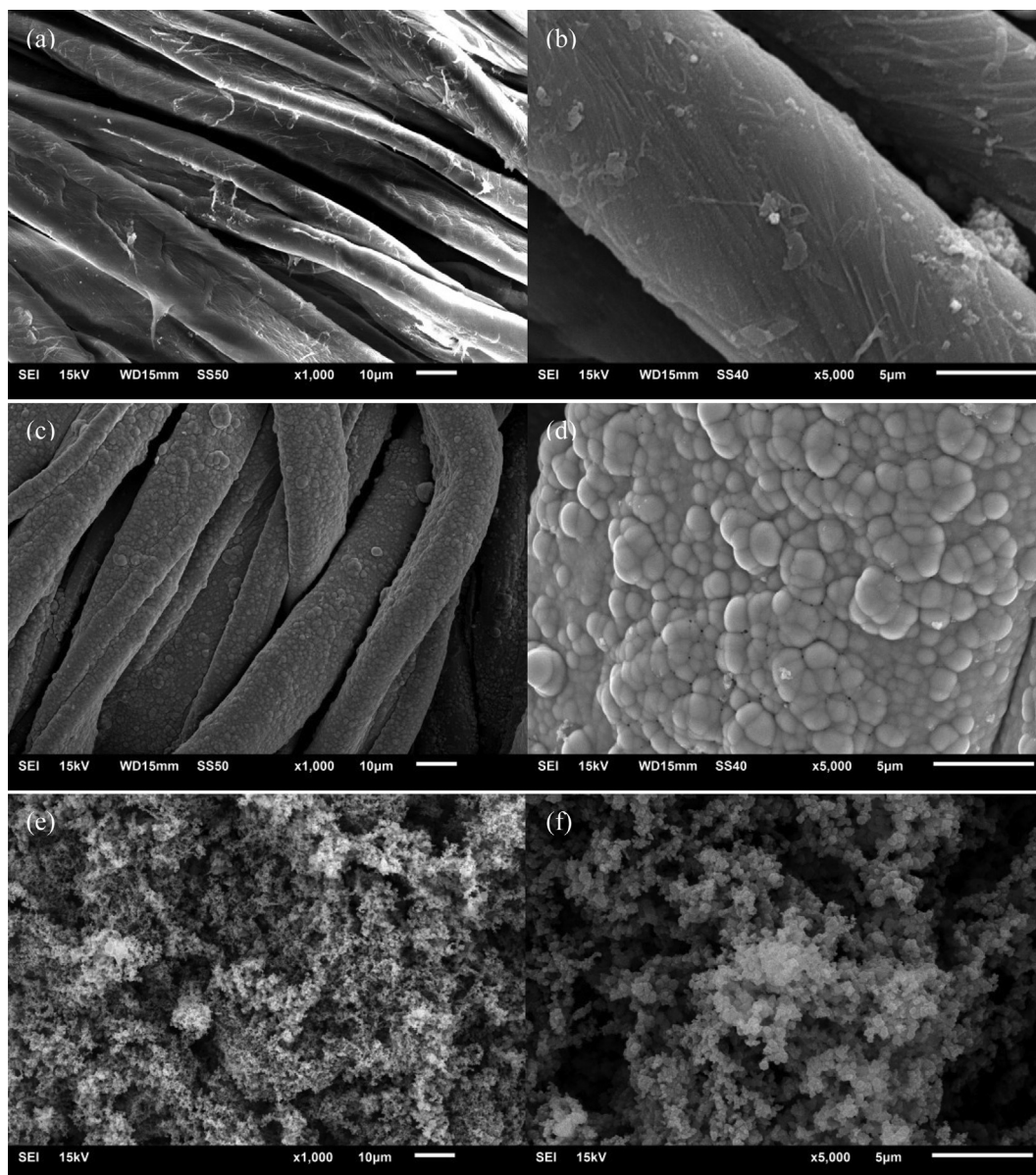


Fig. 1. SEM images. (a) and (b) uncoated cotton fabric; (c) and (d) the Ni-coated cotton fabric; (e) and (f) the PPY/Ni-coated fabric.

### 3. Results and discussion

Fig. 1 shows the SEM surface morphologies of the uncoated and coated cotton fabrics. It can be seen the surface of the uncoated fabric is relatively clean and smooth. After electroless plating, the surface of the sample was fully covered by the Ni coating, which is compact and continuous. There are no obvious flaws or apertures on the coating, and the appearance of cauliflower-like nodule with diameter of about 1–3  $\mu\text{m}$  is distinctly observed. For the PPY/Ni-coated fabric, the boundary of the fiber and the cauliflower-like structure of the Ni coating could not be found, and the PPY layer is quite loose and well formed as a three-dimensional network of small conducting granular particles on the fiber and fabric surfaces.

The chemical composition of the Ni-coated fabric was analyzed by the EDS spectrum as shown in Fig. 2a. The C and O elements are from air, while the Ni and P peaks are attributed the electroless coating. It is known that the beginning of the electroless Ni

deposition is controlled by the anodic process and the first step involves the adsorption of hypophosphite on the catalytic surface. Under the catalytic action of metallic Ni clusters on the fabric surface formed during the sensitization, Ni(II) ions are deposited onto the catalytic surface by capturing electrons furnished by reducing agent ( $\text{H}_2\text{PO}_2^-$ ) via the following chemical reaction in alkaline media:



In this reaction, the adsorption of hypophosphite on the catalytic surface is followed by the hemolytic breakdown of P–H bond.  $\text{H}_2\text{PO}_2^-$  is easily released electrons and oxidized to yield orthophosphorus. Ni(II) ions in the electroless solution are reduced by the electrons generated through the oxidation of the  $\text{H}_2\text{PO}_2^-$ . During the electroless Ni deposition process, phosphorus is codeposited with nickel. The Ni and P contents on the cotton fabric are 97.01 and

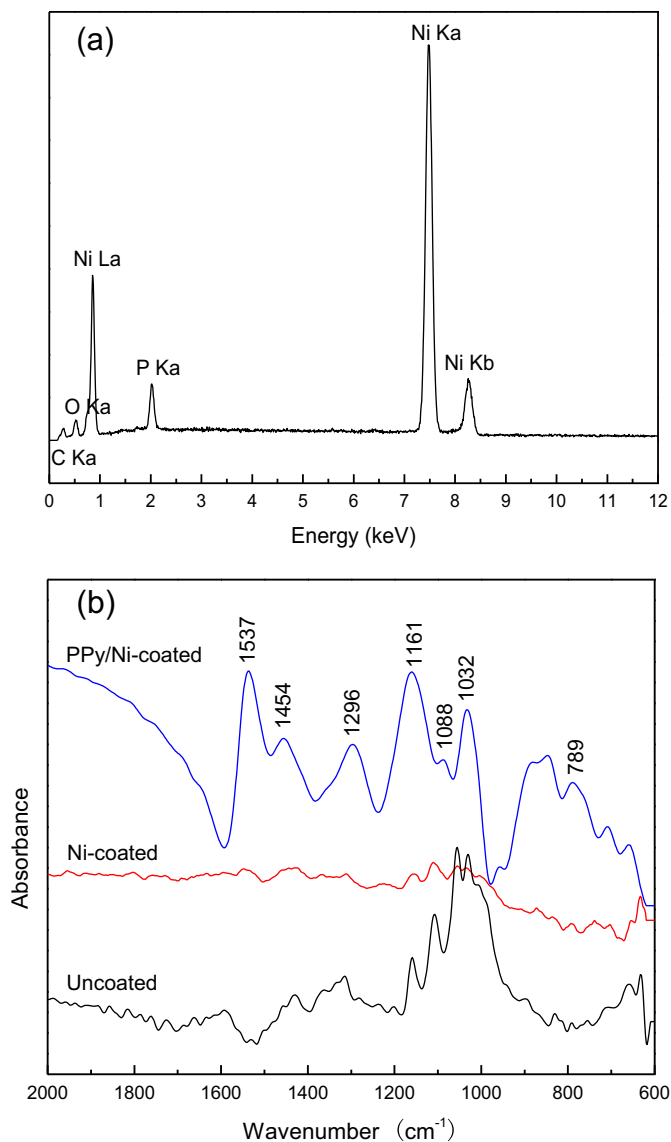


**Fig. 2.** (a) EDS analysis of the Ni-coated fabric; (b) FTIR spectra of the uncoated and coated fabrics.

2.99 wt%, respectively. The percentage phosphorus on the cotton fabric is significantly lower than that on the polyester fabric [25], probably due to the higher concentration of  $\text{NiSO}_4$  used in the present study.

The ATR-FTIR spectra of the uncoated and coated fabrics are shown in Fig. 2b. In the case of the uncoated fabric, the peak at  $1159\text{ cm}^{-1}$  is assigned to the C–O antisymmetric bridge stretching. The strong and sharp bands at  $1055$  and  $1030\text{ cm}^{-1}$  are attributed to the C–O and C–O–C functional groups of the pyranose ring skeletal vibration [26]. After electroless plating, the characteristic absorption bands attributed to cellulose disappeared. Since the infrared beam of the ATR technique analyses only a thin layer of the fiber surface, the absence of the cellulose bands for the Ni-coated fabric further confirms that the fibers are entirely and compactly covered by the Ni coating, and that the thickness of the coating reaches at least several micrometers. The spectrum of the PPy/Ni-coated fabric is characterized by the typical features of PPy [27]. In the range of  $4000\text{--}1600\text{ cm}^{-1}$  there is the characteristic tail of the electronic absorption related to the electrical

conductivity of PPy [27] (only the beginning of this band is shown in Fig. 2b). The broad bands at  $1537\text{ cm}^{-1}$  and  $1454\text{ cm}^{-1}$  are assigned to the C–C and C–N stretching vibrations in pyrrole ring, respectively. The band at  $1296\text{ cm}^{-1}$  is attributed to the C–H and C–N in-plane deformation modes. The peak at  $1161$  is attributed to the breathing vibration of the pyrrole ring. The weak peak at  $1088\text{ cm}^{-1}$  is assigned to the in-plane deformation vibration of  $\text{NH}^+$  groups which are formed in the PPy chains by protonation [27]. The band of N–H in-plane deformation vibration is situated at  $1032\text{ cm}^{-1}$ . Finally, the peak at  $789\text{ cm}^{-1}$  is attributed to C–H out-of-plane ring deformation.

The sheet resistance of the Ni-coated fabric measured by four point probe showed excellent conductivity of  $1.5\text{ }\Omega\text{ sq}^{-1}$ , which is better than that of FTO glasses. After PPy deposition, the sheet resistance of the sample was increased to about  $41.5\text{ }\Omega\text{ sq}^{-1}$ . Ni was selected as the conducting material on cotton fabrics because it has no significant reaction with iodole electrolytes [20] and can be easily coated on fabrics at relatively low temperature. The transmittance of electrolytes did not change remarkably after immersion of the coated fabrics as seen in Fig. 3a. The mechanical adhesion of the coated fabrics was tested by Scotch tape, and no obvious Ni or PPy could be observed on the tape, demonstrating good adhesion of Ni and PPy on the fabric (only the picture for Ni-coated fabric is shown in Fig. 3b). The conductance stability of the PPy/Ni-coated fabric at different curvature (state I–V, the insets) was measured by monitoring the current at a fixed voltage of  $2.0\text{ V}$ . It can be observed that the current was nearly unchanged at different bending states (Fig. 3c), revealing that the conductance of the PPy/Ni-coated fabric is hardly affected by bending stress. These results indicate promising potential of the obtained PPy/Ni-coated fabric in flexible electronics.

To examine the electrochemical characteristics of PPy/Ni-coated fabric and Pt/ITO CE, electrochemical impedance spectroscopy (EIS) measurements were carried out using the symmetrical electrochemical cells of CE/electrolyte/CE configuration. Fig. 4a shows the Nyquist plots of the symmetrical cells. The intersection of high frequency semicircle at real axis represents ohmic series resistance of device ( $R_s$ ), including the sheet resistance of two identical CEs and the electrolytic resistance; the radii of high frequency semicircle corresponds to the charge transfer resistance ( $R_{ct}$ ) at the electrode/electrolyte interface, while the low frequency arc is attributed to the Nernst diffusion impedance ( $Z_W$ ) of the  $\text{I}^-/\text{I}_3^-$  redox couple in a thin layer of electrolyte. The Nyquist plots were fitted using the inset equivalent circuit of Fig. 4a with chi-squared value ( $\chi^2$ , sum of the squares of the residual)  $<10^{-3}$  and the results are shown in Table 1. The  $R_s$  of the PPy electrode is higher than that of the Pt electrode due to no optimization of doping process which affects the conductivity of PPy. The large  $R_s$  can affect the fill factor (FF) of the DSSC based on the fabric CE [28]. The  $R_{ct}$  of the PPy electrode was found to be  $0.50\text{ }\Omega\text{ cm}^2$ , which is even less than of that ( $2.70\text{ }\Omega\text{ cm}^2$ ) of the Pt electrode, indicating a high electrochemical catalytic activity of the PPy CE for the redox process [29]. The CPE represents the capacitance at the interface between the electrode and electrolyte, which can be depicted as

$$Z_{\text{CPE}} = \frac{1}{Y_0(j\omega)^{-\beta}}$$

where  $Y_0$  is the CPE parameter,  $\beta$  is the CPE exponent ( $0 < \beta < 1$ ), and  $\omega$  is the angular frequency. An ideal capacitance has an exact semicircle with a  $\beta$  value of 1. However, surface roughness, porous films, leaky capacitor, and non-uniform current

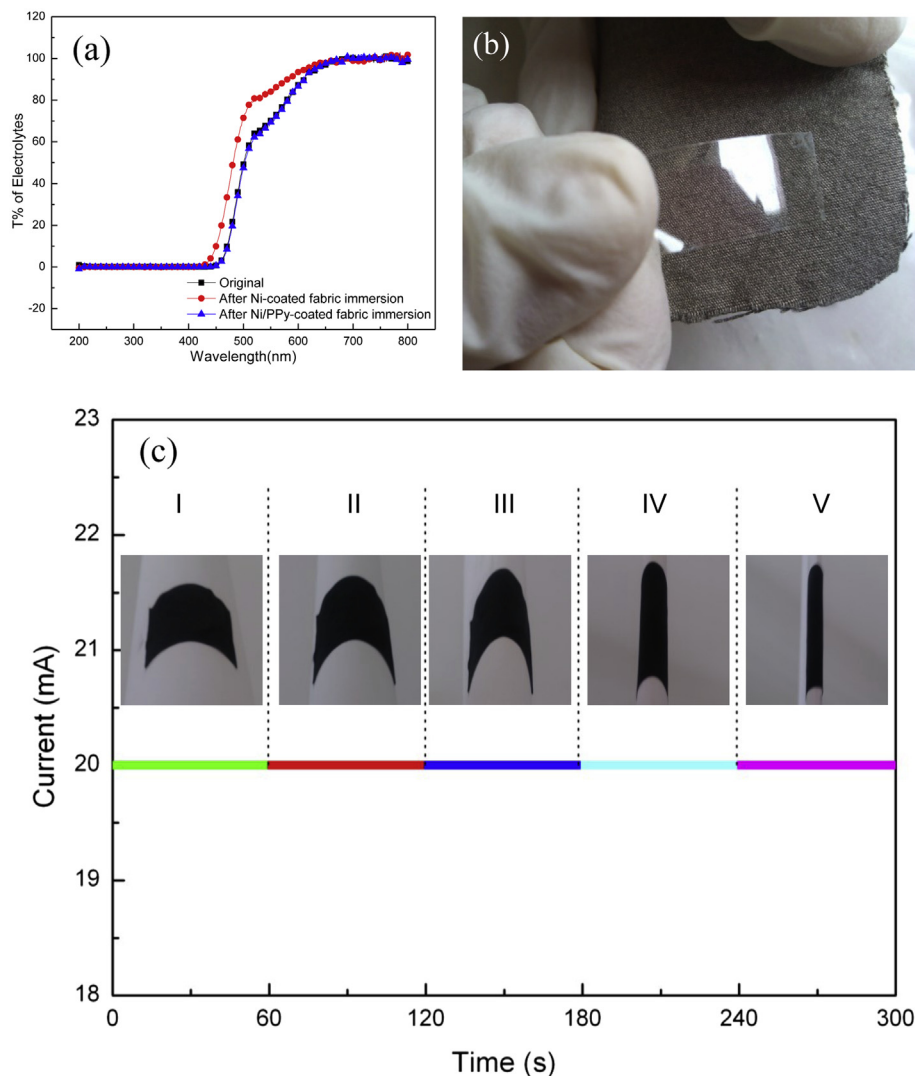


**Fig. 3.** (a) Transmittance of electrolytes before and after the uncoated or coated fabric immersion; (b) the Ni-coated fabric passes the tape test showing the strong adhesion; (c) current–time curves of the PPy/Ni-coated fabric bent with different curvatures under 2.0 V. The upper insets labeled I, II, III, IV and V reveal the five bending states.

distribution can lead to a non-ideal capacitance at the interface of counter electrode and electrolyte, causing the semicircle to depress into an ellipse in the Nyquist plots [30]. This typically causes the  $\beta$  value to decrease below 1. The fitted results show that  $\beta$  of the PPy CE is 0.73, which is smaller than the  $\beta$  value of 0.97 exhibited by the Pt electrode. The lower  $\beta$  value suggests that the PPy CE has a higher porosity than the Pt catalyst [30]. This is consistent with previous work in which the low  $\beta$  value of 0.82 was reported in a highly porous electrospun carbon nanofiber counter electrode [31].

The photovoltaic performance of the DSSCs using the PPy/Ni-coated fabric and Pt-FTO CEs were evaluated under AM 1.5 illumination. The recorded current–voltage ( $J$ – $V$ ) characteristics are shown in Fig. 5. The derived photovoltaic parameters, such as the short-circuit density ( $J_{sc}$ ), open-circuit voltage ( $V_{oc}$ ), fill factor (FF), and overall conversion efficiency ( $\eta$ ) for both the DSSCs are summarized in Table 2. The DSSC with the fabric CE exhibits a  $J_{sc}$  of  $9.60 \text{ mA cm}^{-2}$ , a  $V_{oc}$  of 652 mV, and an FF of 0.52, yielding a  $\eta$  of 3.30%. The corresponding parameters ( $J_{sc}$ ,  $V_{oc}$ , FF, and  $\eta$ ) of the Pt-based DSCs are  $15.10 \text{ mA cm}^{-2}$ , 704 mV, 0.58, and 6.16%, respectively. The unabsorbed light could be reflected back to the photoanode for re-absorption by the semitransparent Pt CE, leading to

a higher  $J_{sc}$  [32–34]. The fabric CE cannot induce such a reflection effect. It is known that  $V_{oc}$  can be related to the  $I_3^-$  concentration using the following equation [35]:

$$V_{oc} = [kT/e] \ln \left\{ I_{inj} / n_{cb} k_{et} [I_3^-] \right\}$$

where  $k$  is the Boltzmann constant,  $T$  is the absolute temperature,  $e$  is an electronic charge,  $I_{inj}$  is the flux of charge resulting from sensitized injection,  $n_{cb}$  is the electron concentration on the surface of  $\text{TiO}_2$ ,  $k_{et}$  is the reaction rate constant of  $I_3^-$  dark reaction on  $\text{TiO}_2$ ,  $[I_3^-]$  is the concentration of  $I_3^-$  in electrolyte. The high concentration of  $I_3^-$  ions at PPy surface gives rise to the low  $V_{oc}$  [17]. The decrement of FF is mainly attributed to the relatively higher sheet resistance of PPy/Ni-coated fabric according to the EIS results. The conductivity of PPy/Ni-coated fabric can be improved by adjusting the chemical synthesis conditions which offers the opportunity to significantly decrease the sheet resistance of PPy/Ni-coated fabric electrode and this study is ongoing. Nevertheless, considering the first set of experiments on employing the PPy-coated fabric as CE for the fabrication of DSSCs, the measured efficiency is respectable.

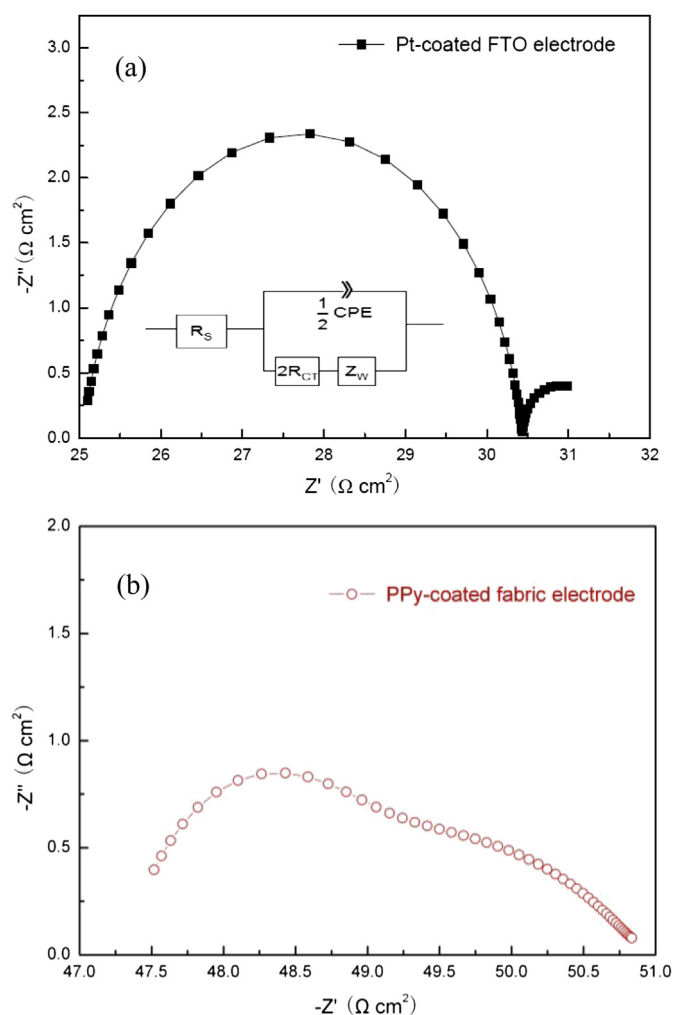


**Fig. 4.** Nyquist plots of the symmetrical cells consisting of two identical (a) Pt electrodes or (b) fabric electrodes. The inset is the equivalent circuit of the symmetrical electrochemical cell for EIS measurements.  $R_s$ : series resistance at the counter electrode. CPE: Constant phase element.  $R_{ct}$ : charge-transfer resistance.  $Z_W$ : Nernst diffusion impedance.

#### 4. Conclusions

In this paper, we have prepared a novel fabric CE for DSSCs using an everyday cotton fabric coated with Ni as substrate and PPy as catalytic material. The fabric CE shows sufficient catalytic activity towards the reduction of  $I_3^-$ . The DSSC fabricated using the fabric CE exhibits power conversion efficiency of 3.30% under AM 1.5 illumination. Our results demonstrate that the PPy/Ni-coated fabric is a promising candidate as Pt-free CE for DSSC fabrication. Furthermore, the flexibility, low weight and low price of the fabric CE would benefit for lowering the production and transportation cost of DSSCs. Our future work will focus on further improvement of the fabric CE for DSSCs by studying the sheet resistance and the assembly method.

**Table 1**

Fitted EIS parameters of the symmetrical cells with the PPy/Ni-coated fabric and Pt-coated FTO electrodes.

Counter electrode	$R_s$ ( $\Omega$ cm <sup>2</sup> )	$R_{ct}$ ( $\Omega$ cm <sup>2</sup> )	$\beta$
Pt-coated FTO	25.04	2.70	0.97
PPy/Ni-coated fabric	47.21	0.50	0.73

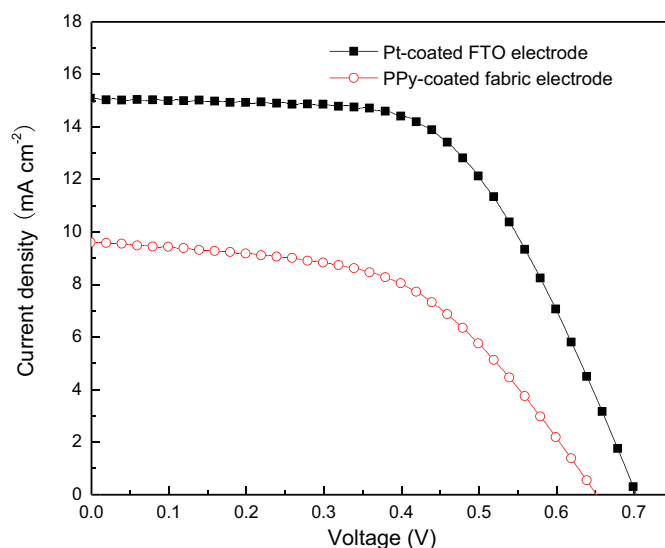


**Fig. 5.** Current–voltage ( $J$ – $V$ ) characteristics of DSSCs employing the Pt-FTO and PPy/Ni-coated fabric counter electrodes measured under AM 1.5 illumination.

**Table 2**

Photovoltaic parameters of DSSCs with the PPy/Ni-coated fabric and Pt-coated FTO CEs.

Counter electrode	$J_{sc}$ (mA cm <sup>−2</sup> )	$V_{oc}$ (mV)	FF	$\eta$ (%)
Pt-coated FTO	15.10	704	0.58	6.16
PPy/Ni-coated fabric	9.60	652	0.52	3.30

#### Acknowledgments

This work was supported by the Natural Science Foundation of China (No. 51003082 and No. 61108033), the Natural Science Foundation of Hubei Province (No. 2012FFA098 and No. 2013CFB064), the Young People Project of Wuhan Science and Technology Bureau (No. 201271031381) and the Science and Technology Research Project of Education Department of Hubei Province (Q20132601).

#### References

- [1] M.K. Nazeeruddin, P. Péchy, T. Renouard, S.M. Zakeeruddin, R. Humphry-Baker, P. Comte, P. Liska, L. Cevey, E. Costa, V. Shklover, L. Spiccia, G.B. Deacon, C.A. Bignozzi, M. Grätzel, *J. Am. Chem. Soc.* 123 (2001) 1613–1624.
- [2] M.K. Nazeeruddin, F.D. Angelis, S. Fantacci, A. Selloni, G. Viscardi, P. Liska, S. Ito, B. Takeru, M. Grätzel, *J. Am. Chem. Soc.* 127 (2005) 16835–16847.
- [3] F. Gao, Y. Wang, D. Shi, J. Zhang, M. Wang, X. Jing, R. Humphry-Baker, P. Wang, S.M. Zakeeruddin, M. Grätzel, *J. Am. Chem. Soc.* 130 (2008) 10720–10728.
- [4] C.-Y. Chen, M. Wang, J.-Y. Li, N. Pootrakulchote, L. Alibabaei, C.-H. Ngoc-le, J.-D. Decoppet, J.-H. Tsai, C. Grätzel, C.-G. Wu, S.M. Zakeeruddin, M. Grätzel, *ACS Nano* 3 (2009) 3103–3109.
- [5] J. Xu, L. Zhu, L. Wang, L. Liu, Z. Bai, L. Wang, W. Xu, *J. Mol. Model.* 18 (2012) 1767–1777.
- [6] J. Xu, L. Zhu, D. Fang, B. Chen, L. Liu, L. Wang, W. Xu, *ChemPhysChem* 13 (2012) 3320–3329.
- [7] X. Wang, J. Xu, M. Li, D. Fang, B. Chen, L. Wang, W. Xu, *RSC Adv.* 3 (2013) 5227–5237.
- [8] K. Imoto, K. Takahashi, T. Yamaguchi, T. Komura, J.-i. Nakamura, K. Murata, *Sol. Energy Mater. Sol. Cells* 79 (2003) 459–469.
- [9] J. Chen, K. Li, Y. Luo, X. Guo, D. Li, M. Deng, S. Huang, Q. Meng, *Carbon* 47 (2009) 2704–2708.
- [10] J.D. Roy-Mayhew, D.J. Bozym, C. Punckt, I.A. Aksay, *ACS Nano* 4 (2010) 6203–6211.
- [11] J. Han, H. Kim, D.Y. Kim, S.M. Jo, S.-Y. Jang, *ACS Nano* 4 (2011) 3503–3509.
- [12] S. Ahmad, J.-H. Yum, X. Zhang, M. Grätzel, H.J. Butt, M.K. Nazeeruddin, *J. Mater. Chem.* 20 (2010) 1654–1658.
- [13] Q. Tai, B. Chen, F. Guo, S. Xu, H. Hu, B. Sebo, X.-Z. Zhao, *ACS Nano* 5 (2011) 3795–3799.

- [14] J. Wu, Q. Li, L. Fan, Z. Lan, P. Li, J. Lin, S. Hao, J. Power Sources 181 (2008) 172–176.
- [15] T. Makris, V. Dracopoulos, T. Stergiopoulos, P. Lianos, Electrochim. Acta 56 (2011) 2004–2008.
- [16] J. Xia, L. Chen, S. Yanagida, J. Mater. Chem. 21 (2011) 4644–4649.
- [17] P. Veerender, V. Saxena, P. Jha, S.P. Koiry, A. Gusain, S. Samanta, A.K. Chauhan, D.K. Aswal, S.K. Gupta, Org. Electron. 13 (2012) 3032–3039.
- [18] C. Bu, Q. Tai, Y. Liu, S. Guo, X. Zhao, J. Power Sources 221 (2013) 78–83.
- [19] J.M. Kroon, N.J. Bakker, H.J.P. Smit, P. Liska, K.R. Thampi, P. Wang, S.M. Zakeeruddin, M. Grätzel, A. Hinsch, S. Hore, U. Würfel, R. Sastrawan, J.R. Durrant, E. Palomares, H. Pettersson, T. Gruszecki, J. Walter, K. Skupien, G.E. Tulloch, Prog. Photovolt. Res. Appl. 15 (2007) 1–18.
- [20] T. Ma, X. Fang, M. Akiyama, K. Inoue, H. Noma, E. Abe, J. Electroanal. Chem. 574 (2004) 77–83.
- [21] M.G. Kang, N.-G. Park, K.S. Ryu, S.H. Chang, K.-J. Kim, Sol. Energy Mater. Sol. Cells 90 (2006) 574–581.
- [22] T. Yamaguchi, N. Tobe, D. Matsumoto, T. Nagai, H. Arakawa, Sol. Energy Mater. Sol. Cells 94 (2010) 812–816.
- [23] S.I. Cha, Y. Kim, K.H. Hwang, Y.-J. Shin, S.H. Seo, D.Y. Lee, Energy Environ. Sci. 5 (2012) 6071–6075.
- [24] C.S. Blackman, C. Piccirillo, R. Binions, I.P. Parkin, Thin Solid Films 517 (2009) 4565–4570.
- [25] R.H. Guo, S.Q. Jiang, C.W.M. Yuen, M.C.F. Ng, G.H. Zheng, J. Coat. Technol. Res. 9 (2012) 171–176.
- [26] G. Liang, L. Zhu, J. Xu, D. Fang, Z. Bai, W. Xu, Electrochim. Acta 103 (2013) 9–14.
- [27] M. Omastová, M. Trchová, J. Kovářová, J. Stejskal, Synth. Met. 138 (2003) 447–455.
- [28] Q. Wang, J.-E. Moser, M. Grätzel, J. Phys. Chem. B 109 (2005) 14945–14953.
- [29] J. Halme, P. Vahermaa, K. Miettunen, P. Lund, Adv. Mater. 22 (2010) E210–E234.
- [30] T.N. Murakami, S. Ito, Q. Wang, M.K. Nazeeruddin, T. Bessho, I. Cesar, P. Liska, R. Humphry-Baker, P. Comte, P. Péchy, M. Grätzel, J. Electrochem. Soc. 153 (2006) A2255–A2261.
- [31] P. Joshi, L. Zhang, Q. Chen, D. Galipeau, H. Fong, Q. Qiao, ACS Appl. Mater. Interfaces 2 (2010) 3572–3577.
- [32] X. Fang, T. Ma, G. Guan, M. Akiyama, T. Kida, E. Abe, J. Electroanal. Chem. 570 (2004) 257–263.
- [33] W.J. Lee, E. Ramasamy, D.Y. Lee, J.S. Song, ACS Appl. Mater. Interfaces 1 (2009) 1145–1149.
- [34] M. Wang, A.M. Anghel, B. Marsan, N.-L.C. Ha, N. Pootrakulchote, S.M. Zakeeruddin, M. Grätzel, J. Am. Chem. Soc. 131 (2009) 15976–15977.
- [35] S.Y. Huang, G. Schlichthörl, A.J. Nozik, M. Grätzel, A.J. Frank, J. Phys. Chem. B 101 (1997) 2576–2582.